

Structural studies of CNG repeats

Agnieszka Kiliszek and Wojciech Rypniewski*

Institute of Bioorganic Chemistry, Polish Academy of Sciences, Noskowskiego 12/14, 61–704 Poznan, Poland

Received November 27, 2013; Revised May 14, 2014; Accepted June 2, 2014

ABSTRACT

CNG repeats (where N denotes one of the four natural nucleotides) are abundant in the human genome. Their tendency to undergo expansion can lead to hereditary diseases known as TREDs (trinucleotide repeat expansion disorders). The toxic factor can be protein, if the abnormal gene is expressed, or the gene transcript, or both. The gene transcripts have attracted much attention in the biomedical community, but their molecular structures have only recently been investigated. Model RNA molecules comprising CNG repeats fold into long hairpins whose stems generally conform to an A-type helix, in which the non-canonical N-N pairs are flanked by C-G and G-C pairs. Each homobasic pair is accommodated in the helical context in a unique manner, with consequences for the local helical parameters, solvent structure, electrostatic potential and potential to interact with ligands. The detailed three-dimensional profiles of RNA CNG repeats can be used in screening of compound libraries for potential therapeutics and in structure-based drug design. Here is a brief survey of the CNG structures published to date.

INTRODUCTION

Trinucleotide repeats (TNRs) are a class of microsatellite sequences abundant in the intergenic as well as genetic regions, including open reading frames. More than 30 000 TNRs (six repeated units or more) have been found in the human genome (1). Similar to other microsatellites, TNR sequences exhibit high variability in length between individuals. The mutability of length and its overrepresentation in genes suggest that these can be regulatory elements or a source of evolutionary change, perhaps fine-tuning gene expressions (2). These TNR features can be functional in a normal organism, but they can become deleterious when abnormal lengthening of repeat units occurs. This is observed in humans with neurological diseases known as TREDs (trinucleotide repeat expansion disorders). One major subset of pathogenic TNRs is the CNG repeats, where N represents one of the four natural nucleotides. CNG repeats are associated with at least 15 diseases, such

as myotonic dystrophy (DM), Huntington's disease, several spinocerebellar ataxias (SCA) and fragile X mental retardation syndrome (FXS) (3).

The current models of the pathomechanism of TREDs postulate two toxic agents: RNA and protein (4); however, recent reports also speculate about DNA toxicity (see reviews (2,5)). The RNA-mediated mechanism is based on the observation that long CNG repeats are transcribed and included in mRNA. There, they form hairpin structures that exhibit a gain-of-function abnormality by sequestering and accumulating regulatory proteins. This upsets the fine balance of cellular processes (6–8) and results in retention of the RNA and proteins in the nucleus, where they form nuclear foci (see review (9)). The second pathomechanism mostly concerns the toxicity of protein. The mutated protein contains elongated polyglutamine (polyQ) tracts, which result in the misfolding and aggregation of the protein (10). Most polyQ-containing proteins are involved in DNA-dependent regulation of transcription or neurogenesis. Moreover, they participate in multiple intermolecular contacts. Similar to the RNA-mediated mechanism, the polyQ-expanded region induces pathogenic interactions with proteins, leading to the formation of toxic mono- and oligomers. Subsequently, amyloid-like inclusions are formed, sequestering all engaged proteins (9).

In recent reviews, the sharp division of pathomechanisms started to blur and became more complex. In addition to the main mechanism of the development of some TREDs, another parallel toxic path has been suggested to coexist (see reviews (11–13)). This path is associated with bidirectional transcription, which normally results in antisense RNA involved in the regulation of gene expression. In cells affected with TREDs, the antisense transcripts can contain an extended run of CNG repeats complementary to the sense strand. Subsequently, the antisense RNA can undergo repeat-associated non-ATG (RAN) translation that occurs independently of an ATG initiation codon (14–16). The small expanded peptides can exhibit toxicity, similar to polyQ diseases. Another possibility is that antisense RNA can hybridize to sense RNA and form double-stranded structures, which can be processed into siRNA, derived from triplet repeats, activating the silencing mechanism (17,18). We cannot exclude that such RNAi is also generated from the hairpins formed by sense CNG transcripts (19–21). Bidirectional transcription is also associ-

*To whom correspondence should be addressed. Tel: +48 61 8528503; Fax: +48 61 8520532; Email: wojtekr@ibch.poznan.pl

ated with a path of DNA toxicity, and the convergent transcription from both strands triggers cell death (22). The double-bubble, which is formed at the expanded repeats by the collision of the sense and antisense transcription, is necessary for the induction of apoptosis (2).

To summarize, in recent years the pathomechanism of TREDs has been intensely investigated. A range of molecular biology techniques was used in *in vitro* and *ex vivo* systems and in *in vivo* models. Additionally, crystallography made a contribution to the study of TREDs. A number of structures have been reported in the last 10 years, mostly concerning RNA-mediated pathogenesis, and these findings have not yet been summarized. In this review, we present crystallographic models of toxic RNA and give an overall view of the structural features of the CNG repeats. We begin with a short description of the diseases associated with each type of repeat, followed by an introduction into the structural studies, including a short characterisation of the secondary structure of the DNA and/or RNA. Next, all crystallographic reports of RNA-mediated molecules are presented and discussed, which is followed by a description of the NMR and thermodynamic studies.

TOXICITY OF EXPANDED CNG REPEATS

Abnormally expanded CUG repeats are best known for the multiple system dysfunctions that they cause in myotonic dystrophy type 1 (DM1) (23). The mutation leading to DM1 is the expansion of a CTG repeat in the 3'-untranslated region (3'-UTR) of the *dystrophia myotonica* protein kinase (*DMPK*) gene. The normal length of 5–37 CTG repeats is expanded in DM1 to 50–3000 repeats (24) and entails a misregulation of alternative splicing of several developmentally regulated transcripts (25,26). This misregulation is caused by altered interactions of the transcripts with two antagonistic splicing regulators: the CUG repeat binding protein (CUG-BP) (27) and the muscleblind-like (MBNL1) protein (28). The level of MBNL1 decreases as it is sequestered to nuclear foci (29,30), while the level of CUG-BP increases (31).

Elongated CAG repeats are best known to cause the poly-Q diseases, in which toxicity is attributed to malformed proteins derived from the affected genes (32,33). However, recent studies indicate that mutant transcripts can also contribute to pathogenesis (34,35). CAG repeats in transcripts are similar to CUG repeats in their interaction with the splicing regulator MBNL1 (34,36), whose sequestration by CUG tracts causes splicing aberrations leading to DM1 (28,37) and spinocerebellar ataxia type 8 (SCA8) (38). CAG repeats trigger neurodegeneration when introduced into a *Drosophila* SCA3 model (39). In all, expanded CAG repeats are the cause of nine human neurodegenerative disorders, including Huntington's disease and several spinocerebellar ataxias (40).

Expansion of CGG repeats in the 5'-untranslated region (5'-UTR) of the fragile X mental retardation gene (*FMR1*) is associated with several phenotypes of increasingly severe pathology, depending on the extent of elongation (41). The normal range found in the population is 5–54 CGG repeats (41–43), where the upper region of 45–54, defined as the 'grey zone', carries an increased likelihood of pathogenic ex-

pansion in descendants (41,44). Tracts of 55–200 CGGs are premutations and can cause a progressive RNA-mediated neurodegenerative disorder known as fragile X-associated tremor ataxia syndrome (FXTAS) (45,46) in elderly males, while females carrying the permutation are at risk of developing premature ovarian failure (47). More than 200 CGG repeats are full mutations resulting in fragile X syndrome (FXS), the most common inherited mental retardation syndrome in man (48).

CCG repeats are highly overexpressed in exons of the human genome and are typically located in the 5'-UTR or in the translated regions (1). Their role in pathogenesis is relatively obscure compared to the other CNG repeats, but they are found to be associated with three tri-nucleotide disorders: Huntington's disease (49), myotonic dystrophy type 1 (50) and chromosome X-linked mental retardation (FRAXE) (51).

SECONDARY STRUCTURE OF CNG REPEATS

The secondary structure of RNA containing CNG repeats has been investigated extensively using *in vitro* models (for more detail, see reviews (52,53)). The models studied included RNA comprising not only CNG repeats but also transcripts of native mRNA. Digestion by nuclease S1 and ribonucleases T1, T2 and V1 as well as lead cleavage of oligomers comprising 17 CNG repeats indicated that all CNG repeats formed hairpin structures and that these hairpins showed several alternative alignments co-existing under non-denaturing polyacrylamide gel electrophoresis conditions (54). Adding terminal C-G 'clamps' reduced this micro-heterogeneity. CNG hairpins clamped by six C-G pairs showed only one alignment. The hairpins, comprising an odd number of CNG repeats, formed apical loops of four nucleotide (nt) residues, as indicated by susceptibility to nuclease digestion. In the case of odd-numbered repeats, CAG and CCG showed 7-nt loops, while CUG and CGG formed tighter 3-nt loops.

Further biophysical and biochemical studies to ascertain the structural diversity of a wider range of RNA triplet repeats categorized all CNG repeats as 'fairly stable hairpins', of which CGG was the most stable and CCG the least stable (55). Addressing the question of the possibility of CGG repeats forming quadruplexes, the authors found no evidence for their formation and concluded that the properties of CGG repeats did not essentially deviate from those of CUG, CCG and CUG repeats.

A more focussed study was carried out on CAG repeats in transcripts related to human diseases: the spinocerebellar ataxia types 3 and 6 and dentatorubral-pallidoluysian atrophy. The cleavage patterns of the transcripts, obtained by digestion with lead and a variety of ribonucleases, indicated the formation of several variants of a slipped hairpin (56). The study also demonstrated that a single-nucleotide polymorphism found near the CAG repeat modulated the structure. A related paper addressed the effect of naturally occurring 'interruptions' in an expanded CAG repeat in the coding sequence of the spinocerebellar ataxia type 1 (57). The cleavage patterns indicated that the interruptions destabilized the hairpin structure, causing specific bulging and branching. This was proposed to mitigate the onset

of pathogenesis. A similar investigation of CAG-repeat-containing transcripts related to spinocerebellar ataxia type 2 revealed the structure-modulating role of naturally occurring CAA interruptions (58). Single-nucleotide polymorphism was also observed in the CGG repeats in FMR1 gene transcripts. Single AGG interruptions changed the folding of the 5'-UTR fragments, resulting in branched hairpin structures (43).

DNA containing an extended number of CNG repeats forms non-B DNA structures (59), which can occur during replication, translation, recombination and repair. During those processes, the two parental strands are separated and single-stranded DNA structures can be formed. The secondary structure of isolated dCNG repeats has been studied by a variety of methods, such as electrophoretic mobility assay, UV absorbance and chemical or enzymatic digestion (see review (60)). Similar to RNA, all four types of isolated repeats form hairpin structures. The G-rich dCGG repeats also have the potential to form tetraplexes. In the presence of K^+ ions, the d(CG₂G)₂₀ oligomer exhibited increased electrophoretic mobility, suggesting that it formed an intramolecular tetraplex (a hairpin folded in half). This result was confirmed by CD, NMR and UV spectroscopy (59).

To date, there is only one direct line of evidence showing that the DNA hairpin structures are formed *in vivo*. Two distinct zinc finger nucleases (ZNF) were engineered to recognize specifically the stem of a hairpin formed by CAG or CTG repeats (61). The nucleases were expressed in cells containing an extended number of repeats. As a result, a contraction of the repeated sequence was observed, indicating the presence of hairpins. Moreover, nuclease activity was detected only in an active replication state and only in cells harbouring 45 or 102 repeated units.

X-RAY CRYSTALLOGRAPHIC STUDIES

Crystal structures have been published of RNA oligomers containing all four types of CNG repeats.

CUG repeats

The earliest crystallographic study of a trinucleotide repeat targeted the structure of an oligomer comprising six CUG repeats (PDB code 1zev) (62). The authors found that the RNA is double-helical, having overall characteristics of the A-form, in which the C-G and G-C base pairs have U-U 'mismatches' in between (Figure 1A). The non-canonical pairing seemed not to distort the backbone from the A-helix. Closer observations of the inter-strand interactions, in particular the details of the non-canonical base-pairing and the solvent structure, were prevented by an apparent superposition of molecules in the crystal lattice. A different study revealed duplexes of G(CUG)₂C at a resolution of 1.23 Å (Figure 1B, PDB code 3g1p) (63). This RNA was also in the A-form with the helical twist in the typical range of 32–34°. The crystal lattice comprised three duplexes, crystallographically independent but with similar structures, stacked end-to-end to form pseudo-infinite helices. This arrangement is frequently found in crystals of nucleic acids. The most notable features of this structure are

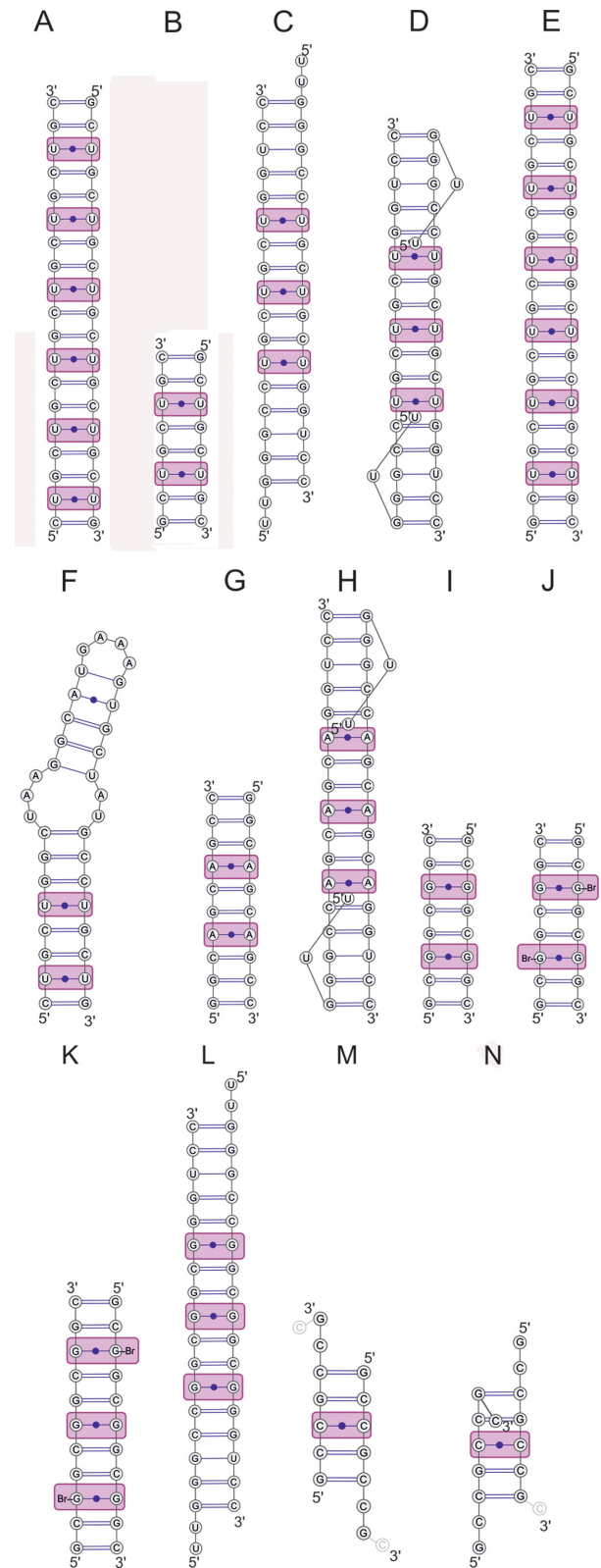


Figure 1. Base-pairing diagrams of the CNG-containing oligomers, whose crystallographic structures have been solved. Structures containing CUG repeats (A–F), CAG (G, H), CGG (I–L) and CCG (M, N) are described in the text.

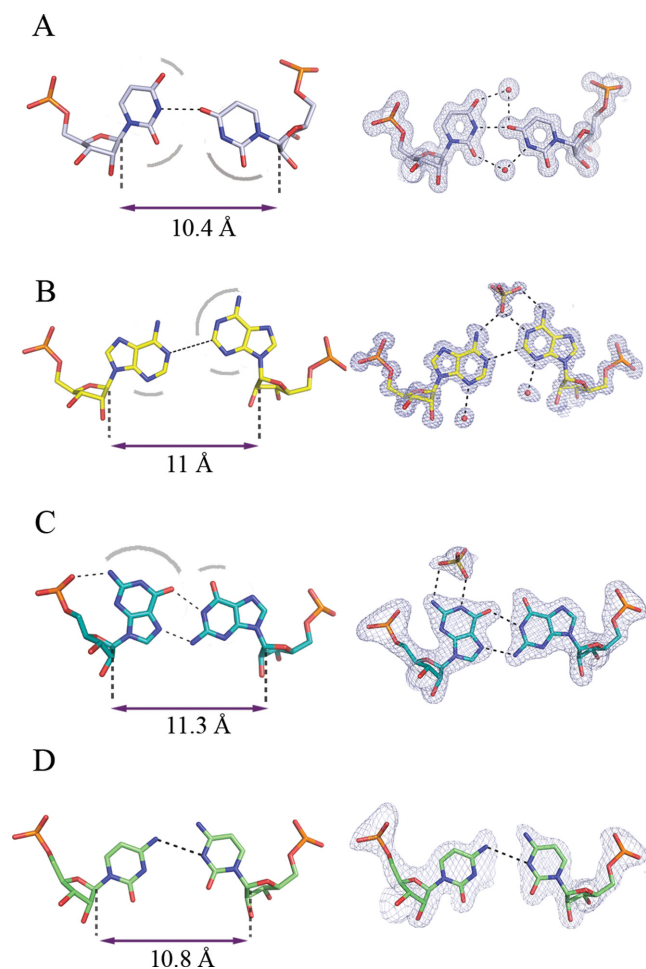


Figure 2. Non-canonical N-N pairs within duplexes formed by CNG repeats: U-U (A), A-A (B), G-G (C) and C-C (D). Strand separation is indicated, measured as a distance between the C1' atoms. Surfaces especially liable to interact with the solvent through H-bonding are indicated with arcs. Representative N-N pairs with the $2F_o - F_c$ electron density, contoured at 1 σ level, are shown (right) based on PDB entries 3g1p, 3nj6, 3r1c, 4e59, respectively.

the clearly resolved interactions within the duplex and the well-defined solvent structure. While the C-G and G-C pairs formed standard Watson-Crick pairing, the U-U pairs interacted in a unique way. The chemical symmetry of the U-U pair is broken in the three-dimensional structure, which has one of the uridines inclined toward the minor groove to make a single hydrogen bond between its carbonyl O4 atom and the N3 amino group of the opposite base (Figure 2A). This interaction appeared 'stretched' compared to the consensus structure derived from previously observed U-U pairs (64) that had two hydrogen bonds. This stretching is clear when the C1'-C1' distance between the two opposite uridine residues is considered. It amounts to 10.4 Å in the context of the CUG repeat, compared to the general consensus of 8.6 Å. A search using FRABASE (65) and FR3D (66) showed stretched U-U pairs in only two other structures: tRNA-Gln, in which the U-U pair closes the anticodon loop, and the A site of 16S rRNA, in which the helix

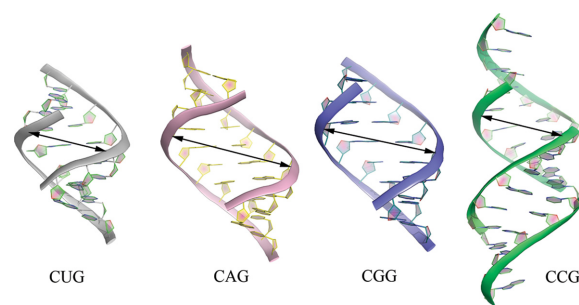


Figure 3. Duplexes containing CNG pairs. Local unwinding and subsequent widening of the major groove can be seen in the vicinity of A-A and G-G pairs.

is flanked by a G-C pair at the 5' side and a C-G pair at the 3' side.

What keeps the uridines apart and prevents them from realising their full base-pairing potential? It is likely that this non-canonical pairing is stabilized by the strong flanking C-G and G-C pairs, which maintain the duplex in a clearly recognisable A-form (Figure 3A). The stability of the U-U pairing is reinforced by ordered water molecules in the major and minor grooves. These waters contribute to the H-bonding network and can be considered a part of the structure. Duplexes comprising CUG repeats have a characteristic pattern of surface electrostatic potential in their minor groove (Figure 4) that comprises alternating bands of positive and negative potential along the direction of the helix axis. The major groove shows no regularity and is predominantly electronegative with positive patches. The hydrogen-bonding potential of the duplexes is demonstrated by their interactions with ordered water molecules and small ligands present in the crystallisation medium (glycerol and sulphate ions). These interactions could be used as a guide in structure-based drug design. The paper also includes a new analysis of the data obtained by Mooers *et al.* (62). After detwining the diffraction intensities, the structure of the [(CUG)₆]₂ duplex (PDB code 3gm7) corresponds closely with the structure of the shorter duplexes.

Given that each U-U pair has two possible conformations, depending on which uridine is inclined, it begs the question: is the choice random or is there a correlation between the conformations of adjacent pairs? The structures included in this study indicate that there is no correlation. This means that despite the chemical symmetry and the palindromic nature of duplexes comprising CUG repeats, the number of possible conformations is large and grows rapidly for longer runs: approximately as $2^N/2$ for N repeats. The authors suggested this as a way of explaining how long runs of CUG repeats could differ from short runs and condense into nuclear foci, as opposed to shorter repeat sequences that remain soluble.

Another study of a crystal structure containing CUG repeats reported a wider range of conformations of the U-U pairs, including arrangements with zero, one or two H-bonds (67). Two crystal forms were reported of a double-stranded construct containing three CUG repeats and 5'UU dangling ends (Figure 1C, D; PDB codes 3syz, 3syw). In both crystal forms, the central CUGs had the uracil

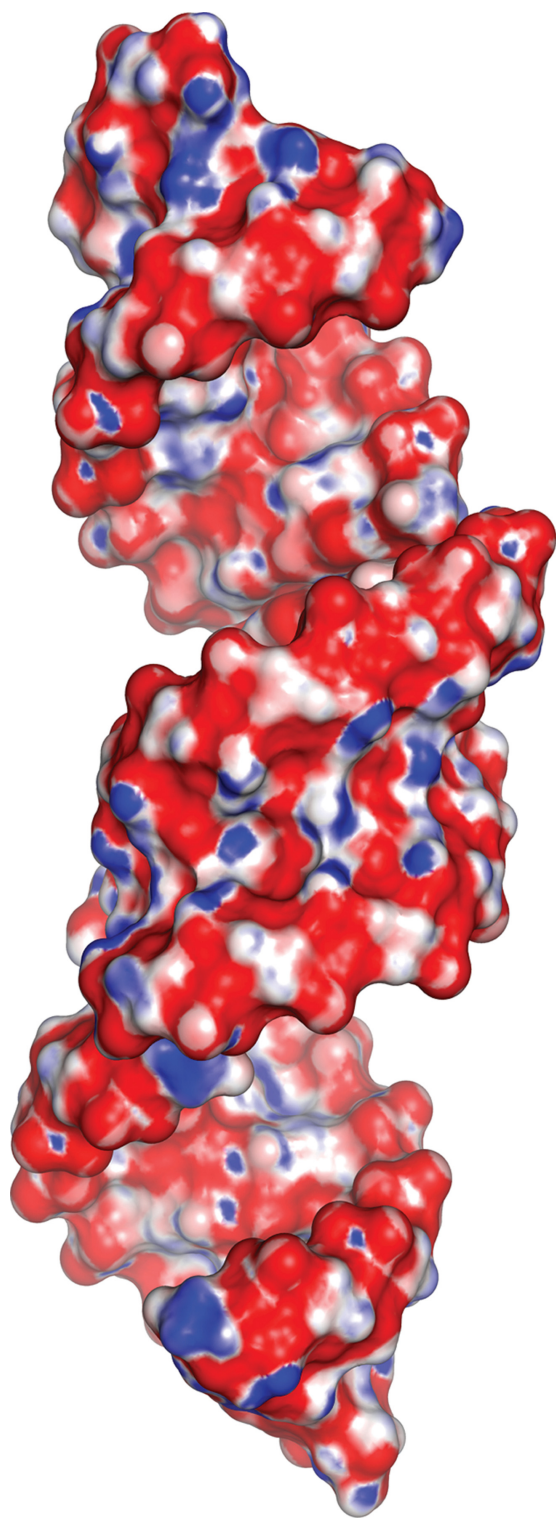


Figure 4. Electrostatic surface potential of three consecutive (GCUGCUGC)₂ duplexes. Red is negative, blue is positive. The minor groove shows a striped pattern of surface potential characteristic of CNG repeats. Based on PDB entry 3gm7.

rings symmetrically opposed and apparently too far apart to form any H-bonds. In the flanking repeats, the two structures differed. In one of them, the first U-U pair formed a single O4-N3 H-bond, while the other pair made a tenuous 3.6 Å contact. The distance between the RNA strands was at least 10 Å and the dangling ends interacted with neighbouring duplexes to form a crystal lattice of pseudo-infinite helices. In the other crystal form, the dangling ends were tucked in the major groove and the width of the groove was increased, while the distance between the strands decreased below 10 Å, which allowed the interacting uridines to form two hydrogen bonds. Based on the structural variation in the crystal, the authors postulated that the U-U pairs could sample multiple conformations *in vivo*, which has implications for the recognition by proteins and small ligands.

A crystal structure of G(CUG)₆C 20-mers forming blunt-ended double helices was described recently (Figure 1E) (68). The crystal lattice contained two distinct duplexes of which one was located on a crystallographic 2-fold axis (PDB code 4e48). Thus, the structure contained nine distinct double-helical CUG repeats. The authors took the opportunity to compare the nine U-U pairs, analyse the spread of conformations and thus gain insight into the dynamics of such pairing. They found that the ‘stretched U-U wobble’ with a single H-bond and associated semi-conserved water structure was the predominant mode of U-U pairing (7 instances), but they also found interesting deviations. One U-U pair exhibited a clearly symmetric pairing mode, described as ‘symmetric H-nonbonded U-U pairing’, which the authors proposed as an intermediate conformation between two predominant asymmetric pairings. The different modes of interactions displayed by the U-U pairs could result in the adaptability of CUG repeats in the protein-bound state. The authors concluded that ‘generally speaking, the U-U pairs just follow the requirements of the system’.

The most recent report regarding the CUG series presents the crystal structure of an RNA construct containing a tandem GAAA tetraloop and its receptor that form the tip and the upper part of a hairpin, respectively, while the lower part of the stem is a double-helical segment of two CUG repeats (Figure 1F, PDB code 4fnj) (69). The combination of the tetraloop with the receptor facilitated crystallisation, which enabled the examination of yet another instance of two consecutive CUG repeats. They formed a helix whose geometry also corresponded to the A-form. The C-G and G-C pairs were standard Watson-Crick pairs, while the two U-U pairs displayed two of the previously observed conformations: one with one hydrogen bond and one with two. The authors catalogued all U-U conformations observed to date and observed that the most common U-U pairing in the context of CUG repeats was the one with one H-bond and a strand separation of at least 10 Å, consistent with the geometry of the A-form. The authors concluded that ‘U-U pairs are dynamic’. This is an understandable statement, but it requires some caution. One could postulate that the multiple conformations are ‘snapshots’ of a dynamic system, but in crystallography, we do not actually observe the transitions between the different instances and therefore cannot be clear about their nature—in particular, their frequency and the conditions upon which they depend.

CAG repeats

Two crystal forms of $(\text{GGCAGCAGCC})_2$ have been reported (70). One of the structures was solved at atomic resolution (0.95 Å) and contained a duplex with the two strands related by crystallographic symmetry (Figure 1G, PDB code 3nj6). The other structure was analysed at medium resolution (1.9 Å) and contained three crystallographically independent duplexes (PDB code 3nj7). All duplexes were closely superposable and possessed general characteristics of the A-form. The A-A pairs, embedded between the canonical C-G and G-C pairs, had both residues in the *anti* conformation (Figure 2B). Clashing between the large purine rings was avoided by shifting of the residues towards the major groove. One was shifted more than the other and this was described as the 'thumbs-up' conformation. The mutual positioning of the adenines allowed one weak C2H2...N1 hydrogen bond. To our knowledge, such pairing between adenosine residues had not been described. The non-canonical character of the interaction resulted in local distortions of the helix geometry – in particular, in the flipping of the O5' atom of the backbone of the neighbouring guanosine, due to a rotation of the C5'-O5' bond. This resulted in a local unwinding of the helix. Although accommodation of the bulky adenine rings within the helical context seems to be 'sterically demanding', the inter-strand C1'-C1' distances (11 Å) for the adenines were only slightly larger than average for the A-form. The unsaturated H-bonding potential of the A-A pair (both *exo*-amino groups and one N1 atom) was externalized in the major groove where it attracted a sulphate anion from the crystallisation medium. Patches of positive potential on the predominantly negative interior of the major groove were clearly visible on the surface electrostatic potential. The minor groove displayed a similar banded pattern of alternating positive and negative potential, similar to that seen in CUG repeats.

In another study, three consecutive CAG repeats within flanking sequences were described (Figure 1H) (71). The middle A-A pair had both adenines in the *anti* conformation and the two adenine rings were modelled as being symmetrically opposed with the N1 atoms and the C2H2 groups in unlikely close contact. Examination of the electron density (see Appendix), calculated on the basis of structure factors deposited by the authors in the PDB (accession code 4j50), indicates disorder, which could be modelled as two alternative conformations of the A-A pair. In each of the conformations, one adenine would be at more of an incline than the other, so that C2H2 would be opposite N1 and a hydrogen bond could form between them, similar to the structures reported before (70). Uninterpreted electron density in the major groove near the A-A pair could indicate a sulphate ion interacting with the *exo*-amino groups, like in the previous paper. The flanking A-A pairs were described as *syn-anti*. The adenine in the *anti* conformation has clear electron density, while the residue in the *syn* conformation appears to be rather disordered. There are significant residual peaks in the difference electron density map associated with the adenine ring, and the sugar-phosphate backbone is weak in this region. It is not clear how this should be modelled. The adenosine in the *syn* conformation seems to

interact with the overhanging disordered uridine from the opposite strand that is tucked in the major groove.

CGG repeats

Three crystal structures of short CGG-containing oligomers have been published (Figure 1I-K) (72). A duplex of $\text{G}(\text{CGG})_2\text{C}$ crystallized with a remarkable 18 distinct duplexes in the unit cell, all arranged in the typical end-to-end manner, in semi-infinite columns (PDB code 3r1c). The other two crystal structures contained guanosine residues brominated at position 8 (PDB codes 3r1d and 3r1e). All helices had the A-form, with some local deviations. In all G-G pairs, one guanosine was *syn* and the other was *anti*, with two hydrogen bonds between the Watson-Crick edge of $\text{G}(\text{anti})$ and the Hoogsteen edge of $\text{G}(\text{syn})$: O6...N1H and N7...N2H (Figure 2C). This type of interaction is common for G-G pairs and has been observed in many NMR and crystallographic structures. The $\text{G}(\text{syn})$ residues also showed unusual α and γ backbone torsion angles, which resulted in a local unwinding of the helix, which seemed to be compensated for elsewhere (Figure 3C). The $\text{G}(\text{syn})$ - $\text{G}(\text{anti})$ pairs had a characteristic hydration pattern and, in addition, attracted charged species from the solvent, especially to the exposed Watson-Crick edges in the major groove. Sulphate anions and hydrated calcium ions, present in the crystallisation medium, interacted with the paired residues. The *syn-anti* arrangement avoids a steric clash of the two bulky guanines within the helical structure, and the C1'-C1' distance between them (11.3 Å on average) is only slightly longer than that for the canonical C-G and G-C flanking pairs. The brominated guanosines were always in the *syn* conformation, which increased the order of the G-G pair by restricting its conformational freedom. The electrostatic potential surface displayed the already familiar banded pattern of positive and negative character in the minor groove. This is due primarily to the C-G and G-C pairs. The potential in the major groove was irregular and matched the observed affinity for small charged ligands. The observation of duplexes for all CGG-containing structures was somewhat surprising to some researchers, who expected quadruplexes by analogy with DNA.

Another paper described an RNA duplex containing three consecutive CGG repeats with flanking sequences and 5'-UU overhangs (Figure 1L) (73). Overall, the structure of the CGG repeats is similar to that described above (72), with $\text{G}(\text{syn})$ - $\text{G}(\text{anti})$ pairs and unusual torsion angles of the $\text{G}(\text{syn})$ residues, resulting in a local unwinding of the helix (PDB code 3js2). The authors noted that the resultant widening of the major groove and the base-pair inclination near the G-G pairs resembled the A'-form of RNA. They also noted an interesting difference from the structures of other triplet repeats: the lack of ordered ions near the G-G pairs, even though several cations and sulphate anions were present in the crystallisation medium.

CCG repeats

At present, there is one paper reporting the crystallographic structure of CCG repeats (74). It describes two oligomers:

(GCCGCCGC)₂ and (GCCG^LCCGC)₂, in which G^L belongs to the 'locked' (LNA) series (Figure 1M, N). The oligomers formed duplexes in the crystal lattice, and again, the RNA has the A-form, but pairing of the strands was unexpected. In the unmodified oligomer, the strands slipped in the 5' direction (PDB code 4e59), whereas in the LNA-containing oligomer, there was a slippage in the 3' direction (PDB code 4e58). In both cases, the result was to reduce the number of C-C pairs from the expected two, if no slippage had occurred, to one. Nevertheless, three instances of double-stranded CCG triplets were observed: one for unmodified RNA and two in crystallographically independent LNA-containing duplexes. Each of the three observed C-C pairs interacts differently, forming either one weak H-bond or none (Figure 2D). LNA has no apparent effect on helical parameters, but base stacking is increased compared to the native duplex. It seems that C-C pairs contribute little to the stability of the duplex, which is why the system acts to eliminate them by strand slippage. These results are in agreement with the measured thermodynamic fragility of CCG repeats. C-C pairs within other known helical RNA structures are relatively rare, but if present, they also show conformational variability. One of the cytosine residues is shifted to various extents towards the minor groove and different H-bonds are observed between the paired cytosines. The apparent weakness of the C-C interactions also sheds light on the observation that the MBNL1 protein, thought to interact with single strands of RNA, recognizes CCG runs as well as CUG and CAG but not the relatively robustly paired CGG repeats.

NMR STUDIES

There are relatively few published works describing NMR studies of RNA TNRs.

The earliest paper presents an analysis of a 97-long run of CUG repeats in solid state (75). The authors noted the presence of canonical C-G pairs and observed resonances consistent with an A-form helix with a C3'-*endo* sugar pucker and an *anti* conformation of the glycosidic torsion angle. Recent solution NMR work on a single CUG with flanking sequences, to stabilize the duplex form, was also consistent with an A-form geometry with a 3C'-*endo* sugar pucker (PDB codes 2l8c, 2l8u and 2l8w) (76). The line broadening and temperature profile of the spectrum indicated a structurally dynamic U-U pair. When the NMR model was subjected to molecular dynamics simulation, the U-U pair was found to adopt conformations with zero, one or two hydrogen bonds, of which the most stable was the structure with one H-bond. These results are essentially in agreement with the crystallographic studies described above.

One paper describes a study of CGG-repeat RNA in solution (77). One short duplex and two hairpins, each predicted to contain three CGG repeats, were investigated. The duplex gave an ambiguous spectrum and most likely formed longer than predicted, overlapping duplexes. The authors observed no patterns characteristic of quadruplexes. The oligomers designed to fold into hairpins gave spectra indicating that hairpins indeed formed and that the non-canonical G-G pairs were located between flanking C-G and G-C pairs. The G-G pairs appeared dynamic with some

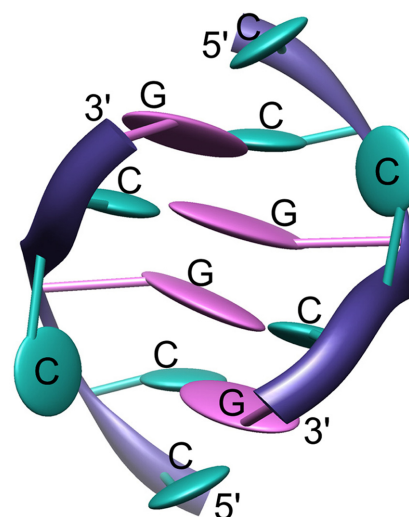


Figure 5. No C-C pairs are formed in the solution NMR structure of (CCGCCG)₂ DNA because the cytosine residues hang out or bulge out of the double helix.

indication of symmetric G-imino–G-imino interactions, but glycosidic bond angles necessary for such an interaction could not be determined due to severe line broadening and signal overlap. The authors again stressed that there was, nevertheless, no evidence of tetraplex formation.

Only one three-dimensional structure has been published of DNA containing CNG repeats (78). The solution structure of d(CCGCCG)₂ was solved using NMR (PDB code 1noq). The double helix contained only G-C and C-G pairs. The C-C pairs were eliminated by strand slippage, which resulted in dangling cytosine residues at the 5' site of each strand. In addition, both 4C residues bulged out causing deformation of the phosphate backbone (Figure 5). The structure shows similarity with the crystallographic models in that the unstable C-C pairs have been eliminated.

THERMODYNAMIC PROPERTIES OF CNG REPEATS VERSUS CRYSTALLOGRAPHIC DATA

Thermodynamic studies have shown that RNA oligomers containing 2–3 repeats form duplexes, while oligomers with 4–5 repeated units exist as a mixture of duplexes and hairpins. Longer RNA molecules form only hairpins (79). Duplexes of G(CNG)_{2–4}C oligomers have comparable thermodynamic stability. Oligomers of CGG repeats have the lowest free energy (ΔG_{37°) (approx. -10 kcal/mol) followed by comparable oligomers of CUG repeats (-7.5 kcal/mol), then CAG \approx CCG (-6.5 kcal/mol). Hairpin structures containing 5–7 CNG units also have comparable stability, but the most stable repeats are CUG, followed by CAG, then CGG and CCG. However, such oligomers form a mixture of structures and deconvolution of the melting curves is necessary to obtain the thermodynamic parameters of each type of structure. The results for longer RNA molecules containing 20 repeats agree with those obtained for shorter oligomers (55). Values of ΔG_{37° range from -2.38 to -6.68 kcal/mol. In 100 mM NaCl, the most thermodynamically stable were CGG, then CAG, CUG and CCG repeats. How-

ever, measurements performed in 100 mM KCl gave different results. The stability series began with CAG repeats followed by CGG, CUG and CCG. The biggest drop in thermal stability was observed for the CGG repeats. The destabilising effect on other TNR RNA was lower: in the range of 0.18–0.69 kcal/mol. The loss of stability in the presence of K^+ ions was also an indication that none of the RNA formed tetraplexes, which are generally promoted by the presence of K^+ .

Thermodynamic stability is an important property of nucleic acids and is difficult to investigate using crystallography, although some estimations are possible based on the number of H-bonds in the N-N pairs or the area of stacking interactions. Considering the aforementioned parameters in the crystallographic structures of TNR RNA, the CGG repeats appear the most stable. The G-G pairs form the largest number of hydrogen bonds (in addition to two H-bonds between the paired guanines, the residue in the *syn* conformation bonds the phosphate group of its own strand). The CUG repeats form the second most stable structure due to the one regular H-bond within the U-U pair. The A-A pairs within the CAG repeats interact *via* one weak C-H...N hydrogen bond. In the case of the CCG repeats, the system limits the number of non-canonical pairs, which do not readily form H-bonds. However, the thermodynamic data for duplexes of (GCUGCUGC)₂ and for (GCCGCCGC)₂ show interesting properties. RNA containing CCG repeats is more stable ($\Delta G_{37^\circ} = -6.09$ kcal/mol) than CUG repeats ($\Delta G_{37^\circ} = -5.08$ kcal/mol). For longer oligomers (3 and 4 repeated units), the stability increases for CUG ($\Delta G_{37^\circ} > 7$ kcal/mol), while for CCG, it remains nearly the same. This effect is difficult to explain, but in the CUG repeats structure, this can be due to limited stacking interactions that increase with oligomer length. In the case of the CCG repeats, this suggests that strand slippage occurs as observed in the crystallographic models. One of the C-C pair is eliminated, giving energetic gain for the short RNA. For longer oligomers, the system is most likely not able to reduce the number of non-canonical pairs destabilising the RNA structure.

Interestingly, in our experience, the ease of crystallisation and the crystal reproducibility of the oligomer corresponded to the thermodynamic properties of the particular type of CNG repeat. The CGG oligomers crystallized rapidly, but it was difficult to obtain monocrystals. Most likely, the conformational flexibility of the G-G pair was introducing disorder that was overcome by seeding. In the case of CUG, good crystals appeared within several days. The oligomers of the CAG and CCG repeats were the most challenging for crystallisation. The crystal reproducibility was random and attempts to optimize crystallisation did not give satisfactory results. It seems that serendipitous changes in the fragile equilibrium in the crystallisation drops enabled us to obtain single crystals.

CONCLUSIONS

All CNG repeats fold into hairpins in which the double-stranded stems have non-canonical N-N pairs that are stabilized by the sturdy C-G and G-C pairs. The A-form prevails albeit with some deviations characteristic of the given N-N

pair. All CNG duplexes have been characterized in crystallographic detail in terms of their base-pairing, interactions with the solvent and small ligands, detailed helical parameters and deviations from the canonical A-helix as well as their electrostatic potential and potential to form hydrogen bonds. Their three-dimensional structural profiles are detailed enough to serve as a basis for screening compound libraries for potentially useful ligands and for structure-based drug design.

PERSPECTIVES

Time has come to move on to more complex structures. To begin with, the picture of hairpins formed by CNG repeats is incomplete. Although detailed structures of their double-stranded stems have been solved, we still do not know the structure of the apical loops. Second, to understand the toxicity of the expanded CNG repeats, one would need to examine their interactions with other molecules and their role in altered gene splicing and the formation of nuclear foci. With this knowledge, one could search in a rational way for ligands that would bind the CNG runs to mitigate their deleterious effects.

This question is addressed in a paper reporting the crystallographic complex of zinc finger domains from the alternative splicing regulator protein MBNL1 and CGCUGU (80). The model shows the protein interacting with a short single-stranded RNA, in particular with the GC step in its sequence. Inspection of the atomic coordinates and the electron density calculated using the structure factors deposited with the PDB (code 3d2s) reveals unexplained degradation of the RNA. From a crystallographer's perspective, it reveals a puzzling, nearly perfect match between pairs of protein molecules and the associated RNA chains, which are related by a translation of half a unit cell along the crystallographic *a*-axis. Further studies are clearly necessary to elucidate the interactions of CNG repeats with their protein partners.

Another clear aim for further studies is a detailed characterisation of complexes between CNG repeats and compounds that could bind them specifically and, hopefully, reverse the precipitation of nuclear foci or prevent their formation. Several classes of compounds have been proposed as potential therapeutics (81–84). Examining their interactions with CNG runs would help verify their utility and enable their refinement.

APPENDIX

Examining the atomic coordinates and the corresponding electron density is a useful addition to reading crystallographic papers, and it can be accomplished easily, even by non-crystallographers. Freely available applications such as Coot (www2.mrc-lmb.cam.ac.uk/Personal/pemsley/cool) automatically download atomic models and calculate electron density maps; one needs only to enter the PDB code to view this information.

FUNDING

National Science Centre [Poland, UMO-2011/01/B/NZ1/04429]. Source of open access

funding: National Science Centre [Poland, UMO-2011/01/B/NZ1/04429].

Conflict of interest statement. None declared.

REFERENCES

- Kozłowski, P., de Mezer, M., and Krzyżosiak, W.J. Kozłowski, P., de Mezer, M., and Krzyżosiak, W.J. (2010) Trinucleotide repeats in human genome and exome. *Nucleic Acids Res.*, **38**, 4027–4039.
- Lin, Y. and Wilson, J.H. Lin, Y. and Wilson, J.H. (2011) Transcription-induced DNA toxicity at trinucleotide repeats: double bubble is trouble. *Cell Cycle*, **10**, 611–618.
- Mirkin, S.M. Mirkin, S.M. (2007) Expandable DNA repeats and human disease. *Nature*, **447**, 932–940.
- Nelson, D.L., Orr, H.T., and Warren, S.T. Nelson, D.L., Orr, H.T., and Warren, S.T. (2013) The unstable repeats—three evolving faces of neurological disease. *Neuron*, **77**, 825–843.
- Polak, U., McIvor, E., Dent, S.Y., Wells, R.D., and Napierala, M. Polak, U., McIvor, E., Dent, S.Y., Wells, R.D., and Napierala, M. (2013) Expanded complexity of unstable repeat diseases. *Biofactors*, **39**, 164–175.
- O'Rourke, J.R. and Swanson, M.S. O'Rourke, J.R. and Swanson, M.S. (2009) Mechanisms of RNA-mediated disease. *J. Biol. Chem.*, **284**, 7419–7423.
- Todd, P.K. and Paulson, H.L. Todd, P.K. and Paulson, H.L. (2010) RNA-mediated neurodegeneration in repeat expansion disorders. *Ann. Neurol.*, **67**, 291–300.
- Echeverria, G.V. and Cooper, T.A. Echeverria, G.V. and Cooper, T.A. (2012) RNA-binding proteins in microsatellite expansion disorders: mediators of RNA toxicity. *Brain Res.*, **1462**, 100–111.
- Wojciechowska, M. and Krzyżosiak, W.J. Wojciechowska, M. and Krzyżosiak, W.J. (2011) Cellular toxicity of expanded RNA repeats: focus on RNA foci. *Hum. Mol. Genet.*, **20**, 3811–3821.
- Almeida, B., Fernandes, S., Abreu, I.A., and Macedo-Ribeiro, S. Almeida, B., Fernandes, S., Abreu, I.A., and Macedo-Ribeiro, S. (2013) Trinucleotide repeats: a structural perspective. *Front. Neurol.*, **4**, 76.
- Budworth, H. and McMurray, C.T. Budworth, H. and McMurray, C.T. (2013) Bidirectional transcription of trinucleotide repeats: roles for excision repair. *DNA Repair (Amst.)*, **12**, 672–684.
- Marti, E. and Estivill, X. Marti, E. and Estivill, X. (2013) Small non-coding RNAs add complexity to the RNA pathogenic mechanisms in trinucleotide repeat expansion diseases. *Front. Mol. Neurosci.*, **6**, 45.
- Sicot, G., Gourdon, G., and Gomes-Pereira, M. Sicot, G., Gourdon, G., and Gomes-Pereira, M. (2011) Myotonic dystrophy, when simple repeats reveal complex pathogenic entities: new findings and future challenges. *Hum. Mol. Genet.*, **20**, R116–R123.
- Ladd, P.D., Smith, L.E., Rabaia, N.A., Moore, J.M., Georges, S.A., Hansen, R.S., Hagerman, R.J., Tassone, F., Tapscott, S.J., and Filippova, G.N. Ladd, P.D., Smith, L.E., Rabaia, N.A., Moore, J.M., Georges, S.A., Hansen, R.S., Hagerman, R.J., Tassone, F., Tapscott, S.J., and Filippova, G.N. (2007) An antisense transcript spanning the CGG repeat region of FMR1 is upregulated in premutation carriers but silenced in full mutation individuals. *Hum. Mol. Genet.*, **16**, 3174–3187.
- Pearson, C.E. Pearson, C.E. (2011) Repeat associated non-ATG translation initiation: one DNA, two transcripts, seven reading frames, potentially nine toxic entities!. *PLoS Genet.*, **7**, e1002018.
- Zu, T., Gibbens, B., Doty, N.S., Gomes-Pereira, M., Huguette, A., Stone, M.D., Margolis, J., Peterson, M., Markowski, T.W., and Ingram, M.A. et al. Zu, T., Gibbens, B., Doty, N.S., Gomes-Pereira, M., Huguette, A., Stone, M.D., Margolis, J., Peterson, M., Markowski, T.W., and Ingram, M.A. (2011) Non-ATG-initiated translation directed by microsatellite expansions. *Proc. Natl. Acad. Sci. U.S.A.*, **108**, 260–265.
- Lawlor, K.T., O'Keefe, L.V., Samaraweera, S.E., van Eyk, C.L., McLeod, C.J., Maloney, C.A., Dang, T.H., Suter, C.M., and Richards, R.I. Lawlor, K.T., O'Keefe, L.V., Samaraweera, S.E., van Eyk, C.L., McLeod, C.J., Maloney, C.A., Dang, T.H., Suter, C.M., and Richards, R.I. (2011) Double-stranded RNA is pathogenic in Drosophila models of expanded repeat neurodegenerative diseases. *Hum. Mol. Genet.*, **20**, 3757–3768.
- Yu, Z., Teng, X., and Bonini, N.M. Yu, Z., Teng, X., and Bonini, N.M. (2011) Triplet repeat-derived siRNAs enhance RNA-mediated toxicity in a Drosophila model for myotonic dystrophy. *PLoS Genet.*, **7**, e1001340.
- Handa, V., Saha, T., and Usdin, K. Handa, V., Saha, T., and Usdin, K. (2003) The fragile X syndrome repeats form RNA hairpins that do not activate the interferon-inducible protein kinase, PKR, but are cut by Dicer. *Nucleic Acids Res.*, **31**, 6243–6248.
- Krol, J., Fiszer, A., Mykowska, A., Sobczak, K., de Mezer, M., and Krzyżosiak, W.J. Krol, J., Fiszer, A., Mykowska, A., Sobczak, K., de Mezer, M., and Krzyżosiak, W.J. (2007) Ribonuclease dicer cleaves triplet repeat hairpins into shorter repeats that silence specific targets. *Mol. Cell*, **25**, 575–586.
- Malinina, L. Malinina, L. (2005) Possible involvement of the RNAi pathway in trinucleotide repeat expansion diseases. *J. Biomol. Struct. Dyn.*, **23**, 233–235.
- Lin, Y., Leng, M., Wan, M., and Wilson, J.H. Lin, Y., Leng, M., Wan, M., and Wilson, J.H. (2010) Convergent transcription through a long CAG tract destabilizes repeats and induces apoptosis. *Mol. Cell Biol.*, **30**, 4435–4451.
- Groenen, P. and Wieringa, B. Groenen, P. and Wieringa, B. (1998) Expanding complexity in myotonic dystrophy. *Bioessays*, **20**, 901–912.
- Brook, J.D., McCurrach, M.E., Harley, H.G., Buckler, A.J., Church, D., Aburatani, H., Hunter, K., Stanton, V.P., Thirion, J.P., and Hudson, T. et al. Brook, J.D., McCurrach, M.E., Harley, H.G., Buckler, A.J., Church, D., Aburatani, H., Hunter, K., Stanton, V.P., Thirion, J.P., and Hudson, T. (1992) Molecular basis of myotonic dystrophy: expansion of a trinucleotide (CTG) repeat at the 3' end of a transcript encoding a protein kinase family member. *Cell*, **68**, 799–808.
- Ranum, L.P. and Cooper, T.A. Ranum, L.P. and Cooper, T.A. (2006) RNA-mediated neuromuscular disorders. *Annu. Rev. Neurosci.*, **29**, 259–277.
- Napierala, M. and Krzyżosiak, W.J. Napierala, M. and Krzyżosiak, W.J. (1997) CUG repeats present in myotonic kinase RNA form metastable “slippery” hairpins. *J. Biol. Chem.*, **272**, 31079–31085.
- Timchenko, L.T., Timchenko, N.A., Caskey, C.T., and Roberts, R. Timchenko, L.T., Timchenko, N.A., Caskey, C.T., and Roberts, R. (1996) Novel proteins with binding specificity for DNA CTG repeats and RNA CUG repeats: implications for myotonic dystrophy. *Hum. Mol. Genet.*, **5**, 115–121.
- Miller, J.W., Urbinati, C.R., Teng-Ummuay, P., Stenberg, M.G., Byrne, B.J., Thornton, C.A., and Swanson, M.S. Miller, J.W., Urbinati, C.R., Teng-Ummuay, P., Stenberg, M.G., Byrne, B.J., Thornton, C.A., and Swanson, M.S. (2000) Recruitment of human muscleblind proteins to (CUG)_n expansions associated with myotonic dystrophy. *EMBO J.*, **19**, 4439–4448.
- Fardaei, M., Rogers, M.T., Thorpe, H.M., Larkin, K., Hamshere, M.G., Harper, P.S., and Brook, J.D. Fardaei, M., Rogers, M.T., Thorpe, H.M., Larkin, K., Hamshere, M.G., Harper, P.S., and Brook, J.D. (2002) Three proteins, MBNL1, MBLL and MBXL, co-localize in vivo with nuclear foci of expanded-repeat transcripts in DM1 and DM2 cells. *Hum. Mol. Genet.*, **11**, 805–814.
- Mankodi, A., Urbinati, C.R., Yuan, Q.P., Moxley, R.T., Sansone, V., Krym, M., Henderson, D., Schalling, M., Swanson, M.S., and Thornton, C.A. Mankodi, A., Urbinati, C.R., Yuan, Q.P., Moxley, R.T., Sansone, V., Krym, M., Henderson, D., Schalling, M., Swanson, M.S., and Thornton, C.A. (2001) Muscleblind localizes to nuclear foci of aberrant RNA in myotonic dystrophy types 1 and 2. *Hum. Mol. Genet.*, **10**, 2165–2170.
- Timchenko, N.A., Wang, G.L., and Timchenko, L.T. Timchenko, N.A., Wang, G.L., and Timchenko, L.T. (2005) RNA CUG-binding protein 1 increases translation of 20-kDa isoform of CCAAT/enhancer-binding protein beta by interacting with the alpha and beta subunits of eukaryotic initiation translation factor 2. *J. Biol. Chem.*, **280**, 20549–20557.
- La Spada, A.R. and Taylor, J.P. La Spada, A.R. and Taylor, J.P. (2010) Repeat expansion disease: progress and puzzles in disease pathogenesis. *Nat. Rev. Genet.*, **11**, 247–258.
- Zoghbi, H.Y. and Orr, H.T. Zoghbi, H.Y. and Orr, H.T. (2009) Pathogenic mechanisms of a polyglutamine-mediated neurodegenerative disease, spinocerebellar ataxia type 1. *J. Biol. Chem.*, **284**, 7425–7429.

34. Ho, T.H., Savkur, R.S., Poulos, M.G., Mancini, M.A., Swanson, M.S., and Cooper, T.A. Ho, T.H., Savkur, R.S., Poulos, M.G., Mancini, M.A., Swanson, M.S., and Cooper, T.A. (2005) Colocalization of muscleblind with RNA foci is separable from mis-regulation of alternative splicing in myotonic dystrophy. *J. Cell Sci.*, **118**, 2923–2933.
35. de Mezer, M., Wojciechowska, M., Napierala, M., Sobczak, K., and Krzyzosiak, W.J. de Mezer, M., Wojciechowska, M., Napierala, M., Sobczak, K., and Krzyzosiak, W.J. (2011) Mutant CAG repeats of Huntingtin transcript fold into hairpins, form nuclear foci and are targets for RNA interference. *Nucleic Acids Res.*, **39**, 3852–3863.
36. Yuan, Y., Compton, S.A., Sobczak, K., Stenberg, M.G., Thornton, C.A., Griffith, J.D., and Swanson, M.S. Yuan, Y., Compton, S.A., Sobczak, K., Stenberg, M.G., Thornton, C.A., Griffith, J.D., and Swanson, M.S. (2007) Muscleblind-like 1 interacts with RNA hairpins in splicing target and pathogenic RNAs. *Nucleic Acids Res.*, **35**, 5474–5486.
37. Mykowska, A., Sobczak, K., Wojciechowska, M., Kozlowski, P., and Krzyzosiak, W.J. Mykowska, A., Sobczak, K., Wojciechowska, M., Kozlowski, P., and Krzyzosiak, W.J. (2011) CAG repeats mimic CUG repeats in the misregulation of alternative splicing. *Nucleic Acids Res.*, **39**, 8938–8951.
38. Daughters, R.S., Tuttle, D.L., Gao, W., Ikeda, Y., Moseley, M.L., Ebner, T.J., Swanson, M.S., and Ranum, L.P. Daughters, R.S., Tuttle, D.L., Gao, W., Ikeda, Y., Moseley, M.L., Ebner, T.J., Swanson, M.S., and Ranum, L.P. (2009) RNA gain-of-function in spinocerebellar ataxia type 8. *PLoS Genet.*, **5**, e1000600.
39. Li, L.B., Yu, Z., Teng, X., and Bonini, N.M. Li, L.B., Yu, Z., Teng, X., and Bonini, N.M. (2008) RNA toxicity is a component of ataxin-3 degeneration in *Drosophila*. *Nature*, **453**, 1107–1111.
40. Orr, H.T. and Zoghbi, H.Y. Orr, H.T. and Zoghbi, H.Y. (2007) Trinucleotide repeat disorders. *Annu. Rev. Neurosci.*, **30**, 575–621.
41. Fu, Y.H., Kuhl, D.P., Pizzuti, A., Pieretti, M., Sutcliffe, J.S., Richards, S., Verkerk, A.J., Holden, J.J., Fenwick, R.G. Jr, and Warren, S.T. et al. Fu, Y.H., Kuhl, D.P., Pizzuti, A., Pieretti, M., Sutcliffe, J.S., Richards, S., Verkerk, A.J., Holden, J.J., Fenwick, R.G. Jr, and Warren, S.T. (1991) Variation of the CGG repeat at the fragile X site results in genetic instability: resolution of the Sherman paradox. *Cell*, **67**, 1047–1058.
42. Dombrowski, C., Levesque, S., Morel, M.L., Rouillard, P., Morgan, K., and Rousseau, F. Dombrowski, C., Levesque, S., Morel, M.L., Rouillard, P., Morgan, K., and Rousseau, F. (2002) Premutation and intermediate-size FMR1 alleles in 10572 males from the general population: loss of an AGG interruption is a late event in the generation of fragile X syndrome alleles. *Hum. Mol. Genet.*, **11**, 371–378.
43. Napierala, M., Michalowski, D., de Mezer, M., and Krzyzosiak, W.J. Napierala, M., Michalowski, D., de Mezer, M., and Krzyzosiak, W.J. (2005) Facile FMR1 mRNA structure regulation by interruptions in CGG repeats. *Nucleic Acids Res.*, **33**, 451–463.
44. Zhong, N., Ju, W., Pietrofesa, J., Wang, D., Dobkin, C., and Brown, W.T. Zhong, N., Ju, W., Pietrofesa, J., Wang, D., Dobkin, C., and Brown, W.T. (1996) Fragile X “gray zone” alleles: AGG patterns, expansion risks, and associated haplotypes. *Am. J. Med. Genet.*, **64**, 261–265.
45. Hagerman, R.J., Leehey, M., Heinrichs, W., Tassone, F., Wilson, R., Hills, J., Grigsby, J., Gage, B., and Hagerman, P.J. Hagerman, R.J., Leehey, M., Heinrichs, W., Tassone, F., Wilson, R., Hills, J., Grigsby, J., Gage, B., and Hagerman, P.J. (2001) Intention tremor, parkinsonism, and generalized brain atrophy in male carriers of fragile X. *Neurology*, **57**, 127–130.
46. Jacquemont, S., Hagerman, R.J., Leehey, M., Grigsby, J., Zhang, L., Brunberg, J.A., Greco, C., Des Portes, V., Jardini, T., and Levine, R. et al. Jacquemont, S., Hagerman, R.J., Leehey, M., Grigsby, J., Zhang, L., Brunberg, J.A., Greco, C., Des Portes, V., Jardini, T., and Levine, R. (2003) Fragile X premutation tremor/ataxia syndrome: molecular, clinical, and neuroimaging correlates. *Am. J. Hum. Genet.*, **72**, 869–878.
47. Sherman, S.L. Sherman, S.L. (2000) Premature ovarian failure among fragile X premutation carriers: parent-of-origin effect?. *Am. J. Hum. Genet.*, **67**, 11–13.
48. Glass, I.A. Glass, I.A. (1991) X linked mental retardation. *J. Med. Genet.*, **28**, 361–371.
49. Zhang, B.R., Tian, J., Yan, Y.P., Yin, X.Z., Zhao, G.H., Wu, Z.Y., Gu, W.H., Xia, K., and Tang, B.S. Zhang, B.R., Tian, J., Yan, Y.P., Yin, X.Z., Zhao, G.H., Wu, Z.Y., Gu, W.H., Xia, K., and Tang, B.S. (2012) CCG polymorphisms in the huntingtin gene have no effect on the pathogenesis of patients with Huntington’s disease in mainland Chinese families. *J. Neurol. Sci.*, **312**, 92–96.
50. Braidia, C., Stefanatos, R.K., Adam, B., Mahajan, N., Smeets, H.J., Niel, F., Goizet, C., Arveiler, B., Koenig, M., and Lagier-Tourenne, C. et al. Braidia, C., Stefanatos, R.K., Adam, B., Mahajan, N., Smeets, H.J., Niel, F., Goizet, C., Arveiler, B., Koenig, M., and Lagier-Tourenne, C. (2010) Variant CCG and GGC repeats within the CTG expansion dramatically modify mutational dynamics and likely contribute toward unusual symptoms in some myotonic dystrophy type 1 patients. *Hum. Mol. Genet.*, **19**, 1399–1412.
51. Gu, Y., Shen, Y., Gibbs, R.A., and Nelson, D.L. Gu, Y., Shen, Y., Gibbs, R.A., and Nelson, D.L. (1996) Identification of FMR2, a novel gene associated with the FRAXE CCG repeat and CpG island. *Nat. Genet.*, **13**, 109–113.
52. Galka-Marciniak, P., Urbanek, M.O., and Krzyzosiak, W.J. Galka-Marciniak, P., Urbanek, M.O., and Krzyzosiak, W.J. (2012) Triplet repeats in transcripts: structural insights into RNA toxicity. *Biol. Chem.*, **393**, 1299–1315.
53. Krzyzosiak, W.J., Sobczak, K., Wojciechowska, M., Fiszer, A., Mykowska, A., and Kozlowski, P. Krzyzosiak, W.J., Sobczak, K., Wojciechowska, M., Fiszer, A., Mykowska, A., and Kozlowski, P. (2012) Triplet repeat RNA structure and its role as pathogenic agent and therapeutic target. *Nucleic Acids Res.*, **40**, 11–26.
54. Sobczak, K., de Mezer, M., Michlewski, G., Krol, J., and Krzyzosiak, W.J. Sobczak, K., de Mezer, M., Michlewski, G., Krol, J., and Krzyzosiak, W.J. (2003) RNA structure of trinucleotide repeats associated with human neurological diseases. *Nucleic Acids Res.*, **31**, 5469–5482.
55. Sobczak, K., Michlewski, G., de Mezer, M., Kierzek, E., Krol, J., Olejniczak, M., Kierzek, R., and Krzyzosiak, W.J. Sobczak, K., Michlewski, G., de Mezer, M., Kierzek, E., Krol, J., Olejniczak, M., Kierzek, R., and Krzyzosiak, W.J. (2010) Structural diversity of triplet repeat RNAs. *J. Biol. Chem.*, **285**, 12755–12764.
56. Michlewski, G. and Krzyzosiak, W.J. Michlewski, G. and Krzyzosiak, W.J. (2004) Molecular architecture of CAG repeats in human disease related transcripts. *J. Mol. Biol.*, **340**, 665–679.
57. Sobczak, K. and Krzyzosiak, W.J. Sobczak, K. and Krzyzosiak, W.J. (2004) Imperfect CAG repeats form diverse structures in SCA1 transcripts. *J. Biol. Chem.*, **279**, 41563–41572.
58. Sobczak, K. and Krzyzosiak, W.J. Sobczak, K. and Krzyzosiak, W.J. (2005) CAG repeats containing CAA interruptions form branched hairpin structures in spinocerebellar ataxia type 2 transcripts. *J. Biol. Chem.*, **280**, 3898–3910.
59. Wells, R.D., Dere, R., Hebert, M.L., Napierala, M., and Son, L.S. Wells, R.D., Dere, R., Hebert, M.L., Napierala, M., and Son, L.S. (2005) Advances in mechanisms of genetic instability related to hereditary neurological diseases. *Nucleic Acids Res.*, **33**, 3785–3798.
60. Mitas, M. Mitas, M. (1997) Trinucleotide repeats associated with human disease. *Nucleic Acids Res.*, **25**, 2245–2254.
61. Liu, G., Chen, X., Bissler, J.J., Sinden, R.R., and Leffak, M. Liu, G., Chen, X., Bissler, J.J., Sinden, R.R., and Leffak, M. (2010) Replication-dependent instability at (CTG)_x(CAG) repeat hairpins in human cells. *Nat. Chem. Biol.*, **6**, 652–659.
62. Mooers, B.H., Logue, J.S., and Berglund, J.A. Mooers, B.H., Logue, J.S., and Berglund, J.A. (2005) The structural basis of myotonic dystrophy from the crystal structure of CUG repeats. *Proc. Natl. Acad. Sci. U.S.A.*, **102**, 16626–16631.
63. Kiliszek, A., Kierzek, R., Krzyzosiak, W.J., and Rypniewski, W. Kiliszek, A., Kierzek, R., Krzyzosiak, W.J., and Rypniewski, W. (2009) Structural insights into CUG repeats containing the ‘stretched U-U wobble’: implications for myotonic dystrophy. *Nucleic Acids Res.*, **37**, 4149–4156.
64. Auffinger, P. and Hashem, Y. Auffinger, P. and Hashem, Y. (2007) SwS: a solvation web service for nucleic acids. *Bioinformatics*, **23**, 1035–1037.
65. Popenda, M., Blazewicz, M., Szachniuk, M., and Adamiak, R.W. Popenda, M., Blazewicz, M., Szachniuk, M., and Adamiak, R.W. (2008) RNA FRABASE version 1.0: an engine with a database to search for the three-dimensional fragments within RNA structures. *Nucleic Acids Res.*, **36**, D386–D391.

66. Sarver, M., Zirbel, C.L., Stombaugh, J., Mokdad, A., and Leontis, N.B. (2008) FR3D: finding local and composite recurrent structural motifs in RNA 3D structures. *J. Math. Biol.*, **56**, 215–252.
67. Kumar, A., Park, H., Fang, P., Parkesh, R., Guo, M., Nettles, K.W., and Disney, M.D. (2011) Myotonic dystrophy type 1 RNA crystal structures reveal heterogeneous 1 × 1 nucleotide UU internal loop conformations. *Biochemistry*, **50**, 9928–9935.
68. Tamjar, J., Katorcha, E., Popov, A., and Malinina, L. (2012) Structural dynamics of double-helical RNAs composed of CUG/CUG- and CUG/CGG-repeats. *J. Biomol. Struct. Dyn.*, **30**, 505–523.
69. Coonrod, L.A., Lohman, J.R., and Berglund, J.A. (2012) Utilizing the GAAA tetraloop/receptor to facilitate crystal packing and determination of the structure of a CUG RNA helix. *Biochemistry*, **51**, 8330–8337.
70. Kiliszek, A., Kierzek, R., Krzyzosiak, W.J., and Rypniewski, W. (2010) Atomic resolution structure of CAG RNA repeats: structural insights and implications for the trinucleotide repeat expansion diseases. *Nucleic Acids Res.*, **38**, 8370–8376.
71. Yildirim, I., Park, H., Disney, M.D., and Schatz, G.C. (2013) A dynamic structural model of expanded RNA CAG repeats: a refined X-ray structure and computational investigations using molecular dynamics and umbrella sampling simulations. *J. Am. Chem. Soc.*, **135**, 3528–3538.
72. Kiliszek, A., Kierzek, R., Krzyzosiak, W.J., and Rypniewski, W. (2011) Crystal structures of CGG RNA repeats with implications for fragile X-associated tremor ataxia syndrome. *Nucleic Acids Res.*, **39**, 7308–7315.
73. Kumar, A., Fang, P., Park, H., Guo, M., Nettles, K.W., and Disney, M.D. (2011) A crystal structure of a model of the repeating r(CG) transcript found in fragile X syndrome. *ChemBiochem*, **12**, 2140–2142.
74. Kiliszek, A., Kierzek, R., Krzyzosiak, W.J., and Rypniewski, W. (2012) Crystallographic characterization of CCG repeats. *Nucleic Acids Res.*, **40**, 8155–8162.
75. Riedel, K., Herbst, C., Hafner, S., Leppert, J., Ohlenschlager, O., Swanson, M.S., Grolach, M., and Ramachandran, R. (2006) Constraints on the structure of (CUG)₉₇ RNA from magic-angle-spinning solid-state NMR spectroscopy. *Angew. Chem. Int. Ed. Engl.*, **45**, 5620–5623.
76. Parkesh, R., Fountain, M., and Disney, M.D. (2011) NMR spectroscopy and molecular dynamics simulation of r(CCGCUGCGG)₂ reveal a dynamic UU internal loop found in myotonic dystrophy type 1. *Biochemistry*, **50**, 599–601.
77. Zumwalt, M., Ludwig, A., Hagerman, P.J., and Dieckmann, T. (2007) Secondary structure and dynamics of the r(CG) repeat in the mRNA of the fragile X mental retardation 1 (FMR1) gene. *RNA Biol.*, **4**, 93–100.
78. Zheng, M., Huang, X., Smith, G.K., Yang, X., and Gao, X. (1996) Genetically unstable CXG repeats are structurally dynamic and have a high propensity for folding. An NMR and UV spectroscopic study. *J. Mol. Biol.*, **264**, 323–336.
79. Broda, M., Kierzek, E., Gdaniec, Z., Kulinski, T., and Kierzek, R. (2005) Thermodynamic stability of RNA structures formed by CNG trinucleotide repeats. Implication for prediction of RNA structure. *Biochemistry*, **44**, 10873–10882.
80. Teplova, M., and Patel, D.J. (2008) Structural insights into RNA recognition by the alternative-splicing regulator muscleblind-like MBNL1. *Nat. Struct. Mol. Biol.*, **15**, 1343–1351.
81. Hu, J., Gagnon, K.T., Liu, J., Watts, J.K., Syeda-Nawaz, J., Bennett, C.F., Randolph, J., Chattopadhyaya, J., and Corey, D.R. (2011) Allele-selective inhibition of ataxin-3 (ATX3) expression by antisense oligomers and duplex RNAs. *Biol. Chem.*, **392**, 315–325.
82. Ofori, L.O., Hoskins, J., Nakamori, M., Thornton, C.A., and Miller, B.L. (2012) From dynamic combinatorial ‘hit’ to lead: in vitro and in vivo activity of compounds targeting the pathogenic RNAs that cause myotonic dystrophy. *Nucleic Acids Res.*, **40**, 6380–6390.
83. Jahromi, A.H., Nguyen, L., Fu, Y., Miller, K.A., Baranger, A.M., and Zimmerman, S.C. (2013) A novel CUG(exp).MBNL1 inhibitor with therapeutic potential for myotonic dystrophy type 1. *ACS Chem. Biol.*, **8**, 1037–1043.
84. Wong, C.H., Fu, Y., Ramisetty, S.R., Baranger, A.M., and Zimmerman, S.C. (2011) Selective inhibition of MBNL1-CCUG interaction by small molecules toward potential therapeutic agents for myotonic dystrophy type 2 (DM2). *Nucleic Acids Res.*, **39**, 8881–8890.